Acta Crystallographica Section D
Biological Crystallography
ISSN 0907-4449

In-situ measurement of rocking curves during lysozyme crystal growth

Fermín Otálora,[a]* José A. Gavira,[a] Bernard Capelle[b] and Juan Manuel García-Ruiz[a]

[a]Laboratorio de Estudios Cristalográficos, Instituto Andaluz de Ciencias de la Tierra, CSIC-Universidad de Granada, Av. Fuentenueva s/n, Granada 18002, Spain, and [b]Laboratoire de Mineralogie-Cristallographie, Université Paris 6, Tour 26, Deuxième Etage, 4 Place Jussieu, 75252 Paris CEDEX 05, France

Correspondence e-mail: otalora@goliat.ugr.es

Received 15 July 1998
Accepted 13 November 1998

The rocking curve of protein crystals contains a lot of useful information concerning crystal quality, most of which is lost owing to the superimposition of spurious features appearing in these fragile materials after growth, during handling and mounting. To minimize such data spoiling, an experimental setup to perform *in situ* X-ray diffraction experiments during crystal growth has been designed. The setup, which includes video observation to allow the correlation of crystal shape, size and growth rate with X-ray data, has been used to assess the mosaicity of tetragonal lysozyme crystals during crystal growth. The full width at half maximum (FWHM) of diffraction peaks collected from these crystals changes during the growth process as a (directly proportional) response to the growth rates and the different development of different domain blocks. These changes in the domain distribution and FWHM with time involve a 'zonation' of the crystals, which show very different rocking curves in different parts of their volume. The rocking curves recorded *in situ* from growing crystals are easier to understand than those from crystals that have suffered even minor handling.

1. Introduction

The quality of protein crystals is becoming an important field in macromolecular crystallography (Helliwell, 1988; Fourme *et al.*, 1995; Snell *et al.*, 1995; Helliwell *et al.*, 1995; Ferrer *et al.*, 1996; Vaney *et al.*, 1996; Riès-Kautt *et al.*, 1997; Otálora *et al.*, 1999). The rocking curve of a protein crystal contains information on the distribution of mosaic blocks, crystal defects and crystal deformations in the crystalline volume, features which are now being clarified by the macromolecular crystallographer. From a practical point of view, the quality of protein crystals is currently the limiting factor for the collection of high-resolution diffraction data sets for structural analysis at synchrotron sources. The spreading of diffracted intensity over wide areas of the reciprocal space gives rise to very low signal-to-noise statistics for weak high-resolution diffraction peaks even using high-brilliance sources.

Protein crystal quality seems to be mostly controlled by the hydrodynamic and mechanical stability of the growth environment, the sample handling and the manipulation needed to prepare the diffraction experiment. This is the motivation for the development in our laboratory of the gel-acupuncture method for protein crystal growth (García-Ruiz *et al.*, 1993, 1995, 1998; García-Ruiz & Moreno, 1994; Moreno *et al.*, 1996; Otálora & García-Ruiz, 1996), a technique which emulates the physical scenario of microgravity crystal-growth experiments and in which crystal handling is minimized by growing the crystals directly inside X-ray capillaries. At the same time,

hydrodynamic stability is maximized through the creation of a diffusive field slowly transporting the precipitating agent towards the protein chamber. Our previous results on mosaicity (LURE station D25b, ESRF ID19; Otálora *et al.*, 1999) and on the resolution limit (LURE station W32, ESRF ID11; Otálora *et al.*, 1996) of space-grown and earth-grown protein crystals indicate the following.

(i) There is no simple direct correlation between mosaicity and resolution limit.

(ii) A very good full width at half maximum (FWHM) ($2.5 \times 10^{-3\circ}$) and resolution limit (1.15 Å) have been observed in space-grown crystals. Slightly higher values ($3.3 \times 10^{3\circ}$ and 1.25 Å) are normal in crystals grown on earth by the gel-acupuncture technique.

(iii) A large influence of mechanical strength on the quality of protein crystals has been observed. This mainly arises from crystal handling and capillary bending, and produces bent and cracked crystals.

(iv) It is possible to grow large protein crystals showing different crystal quality at different parts of the crystal, as long as these parts grow at different rates.

In order to avoid sample-handling artefacts, we performed an experiment to grow protein single crystals by the gel-acupuncture method and to track *in situ* the evolution of crystal quality during crystal growth. A description of the experimental setup and results are presented in this work.

2. Experimental

The experimental setup is based on a modified gel-acupuncture growth reactor (Figs. 1*a* and 1*b*) designed for on-line measurements at the LURE D25b beamline during crystal growth. This reactor allows the simultaneous acquisition of diffraction data, topographic images and video images of the growing crystals without disturbing the growth process. The reactor was built from only two parts by cutting a single block of aluminium, in order to maximize the rigidity-to-weight ratio. These parts are basically a salt reservoir and its cover plate, which also has a bridge-shaped capillary holder. The hardware needed to fix the whole reactor to the X-ray goniometer is built into the salt reservoir. The protein chamber is

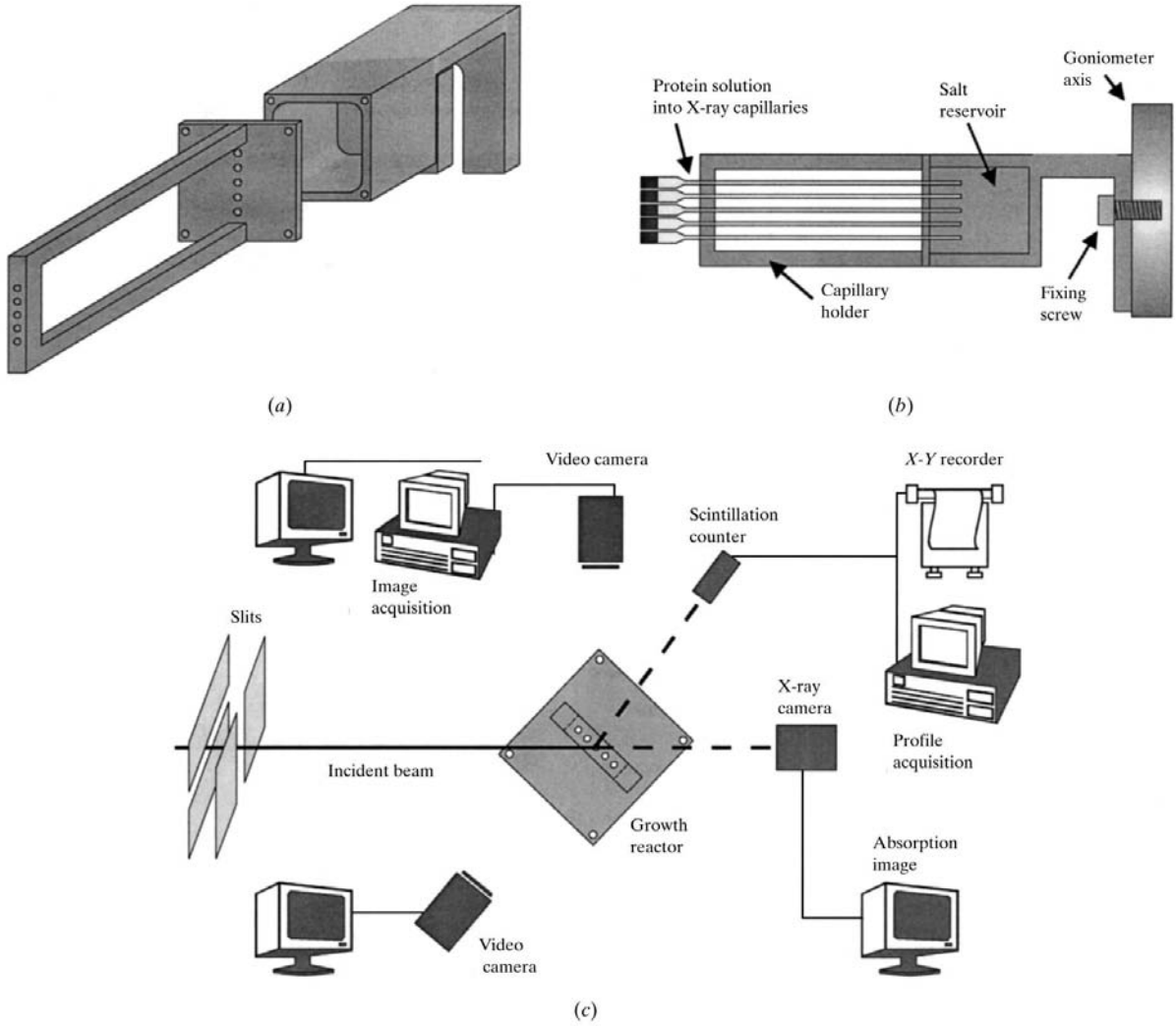

Figure 1
The growth reactor and the experimental setup used for the experiment. (*a*) The growth reactor (see text for description). (*b*) Cross section of the mounted and activated reactor. (*c*) Experimental setup (see text for details).

implemented with up to seven X-ray capillaries containing equal or different protein concentrations. These capillaries are inserted into holes drilled in both the holder bridge and the cover plate and then fixed using small wax drops to avoid any vibration or displacement while sealing the holes of the cover plate. One end of the capillary enters the salt reservoir through the cover plate; the other end is sealed using wax. The salt reservoir contains a gelled solution of the precipitating agent and is hermetically closed by fixing the cover plate to the salt reservoir using four screws. The whole reactor is then fixed to the goniometer axis using a screw.

The experimental setup is schematically shown in Fig. 1(*c*). The capillaries mounted on the sample holder are set in such a way that they are on or very close to the goniometer axis. The whole reactor can be rotated around the axis perpendicular to the paper in Fig. 1(*c*) and translated along the two directions perpendicular to the incident beam: up/down and left/right. A CCD camera is mounted on top of the capillaries for a magnified view of the crystals, which can also be observed using an X-ray sensitive CCD inserted in the direction of the incident beam. The video camera and X-ray camera are adjusted before the experiment in such a way that a crystal is immersed in the beam when it is imaged in focus by the video camera. The monitors attached to these two cameras were marked with the beam position and scale to enable easy crystal positioning and displacement measurement. For this positioning, the two perpendicular movements were used. The up/down movement was used to locate a given capillary in the beam (that is, in focus for the camera lens) and the left/right movement to scan the capillary and set a given crystal under the beam. The video camera is equipped with a zoom which is adjusted to have a field of view covering all the capillaries under observation. This field of view and the initial angular position of the growth reactor are simultaneously adjusted until all the capillaries can be imaged in focus using the up/down displacement. This is necessary because a third movement along the incident beam is not available. A second video camera is set at the bottom for an overall view of the reactor.

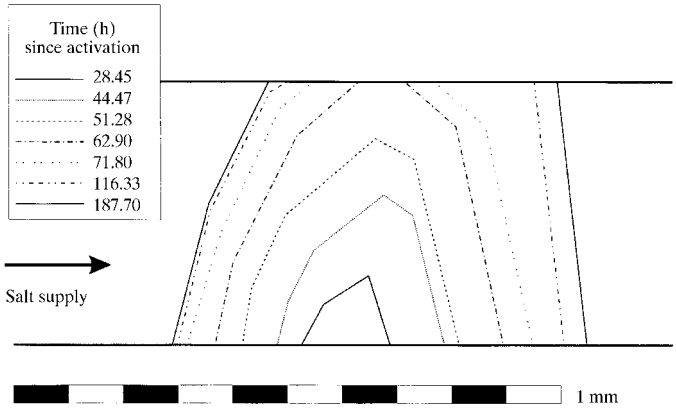

Figure 2
Time sequence of the growth of a single crystal inside a capillary (walls indicated by horizontal lines). After 60 h, the crystal completely fills the capillary, acquiring a round section. After this event, the growth rate of the crystal end facing salt supply is lower than that of the opposite end.

The shape and size of the incident beam can be modified by two perpendicular sets of slits; these changes can be observed in the image of the X-ray camera and translated to the video image by using the marked scales. A scintillation counter connected to an *X*–*Y* recorder and to an automatic digital data-acquisition system are used to record rocking curves.

With this setup, crystal quality (from rocking curves and topography) and growth rate (from video images) can be studied simultaneously without disturbing the growth process. In addition, these studies can be performed during the growth of several different crystals growing from different initial protein concentrations into different capillaries. The experiment is activated when the capillaries are punctuated into the gel. At this moment, the salt starts to diffuse into the capillaries, creating an advancing supersaturation gradient that eventually leads to protein nucleation and crystal growth at different points into the capillaries. Nucleation and crystal growth proceed at a different rate at different parts of each capillary because of the different supersaturation and supersaturation rate (Otálora & García-Ruiz, 1996).

The salt reservoir was filled with a gelled sodium silicate solution containing 10%(*w*/*v*) NaCl. As a protein chamber, we used five X-ray capillaries containing lysozyme solution (Fluka 62971) at different concentrations: 100 mg ml^{-1} (one capillary), 200 mg ml^{-1} (two capillaries) and 300 mg ml^{-1} (two capillaries). The pH of the NaCl solution was adjusted to 6.0 by adding 1 *M* acetic acid. The lysozyme solutions were buffered to pH 4.5 using 50 m*M* sodium acetate. The growth rate was monitored using the top-view video camera connected to an image-acquisition and analysis system. As soon as the crystals nucleated (after 16–24 h), a measurement protocol was started, including periodic measurement of the crystal size and growth rate, the rocking curve of selected

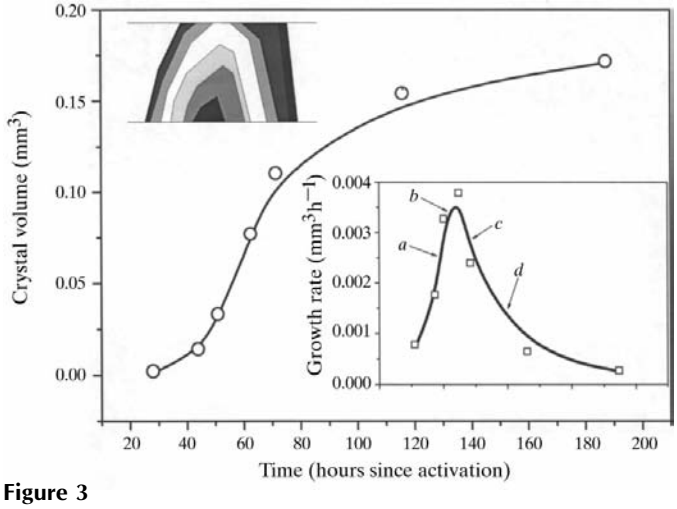

Figure 3
Growth rate of the crystal shown in Fig. 2. The main curve illustrates the crystal volume *versus* time evolution of the crystal (time = 0 is the experiment activation). The curve in the inset shows the growth rate (time derivative of the previous curve). Labels *a*, *b* and *c* in this plot indicate the acquisition time of the rocking curves shown in Figs. 4(*a*), 4(*b*) and 4(*c*). Label *d* indicates the acquisition time of the profile shown in Fig. 5. The top inset shows the spatial distribution of growth rates in the crystal. In this figure, black shading corresponds to 0 mm^3 h^{-1} growth rate and white to the maximum (0.00377 mm^3 h^{-1}) growth rate.

diffraction peaks and (eventually) acquisition of a transmission topography of the crystal.

The experiments were performed at the LURE station D25b, a double-crystal X-ray spectrometer (for more details see Fourme *et al.*, 1995). This beamline was selected on the basis of its excellent facilities for accurately measuring rocking curves and obtaining topographs, such as the very low bandwith, and the possibility of comparing the results obtained with previous experiments (Otálora *et al.*, 1999) without any instrumental correction.

3. Results

Fig. 2 shows the time evolution of the size and shape of a lysozyme single crystal during its growth inside the capillary, as recorded by the video camera on top of the growth reactor. After 60 h, the crystal completely fills the capillary and becomes a cylinder that is still growing at the two ends, though at a lower rate. From this figure it is clear that the growth rate is not uniform during the growth history. In consequence, different parts of the crystal grow at a different rate, producing layers around the initial nucleus. This evolution of growth rates with time and position within the crystal is illustrated in Fig. 3. The curve in the main plot shows the crystal volume, estimated as the scaled crystal projection to the 3/2 power (García-Ruiz & Otálora, 1997). The curve in the inset shows

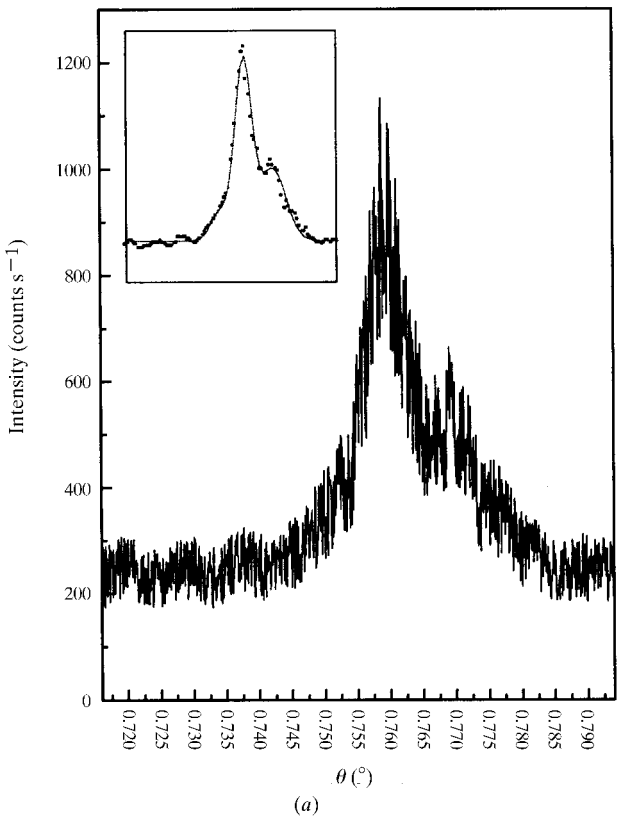

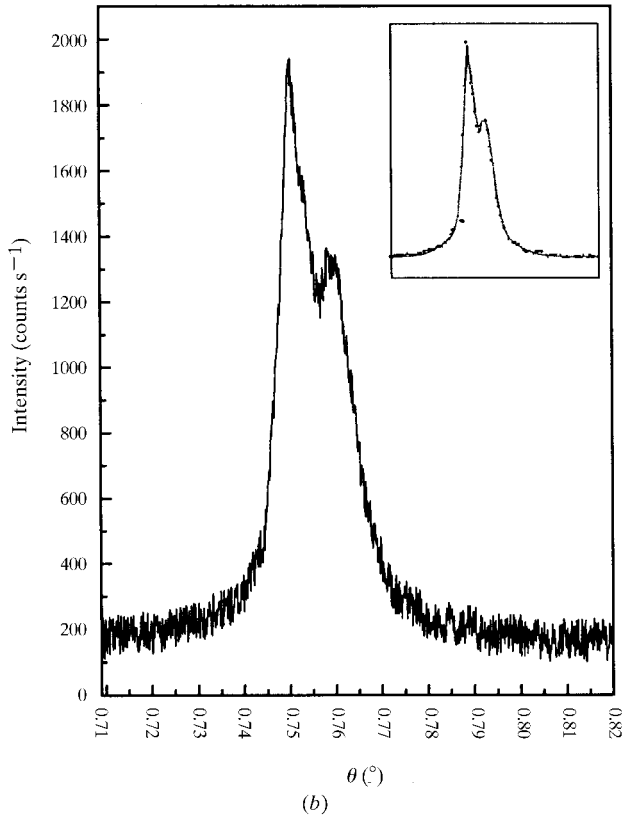

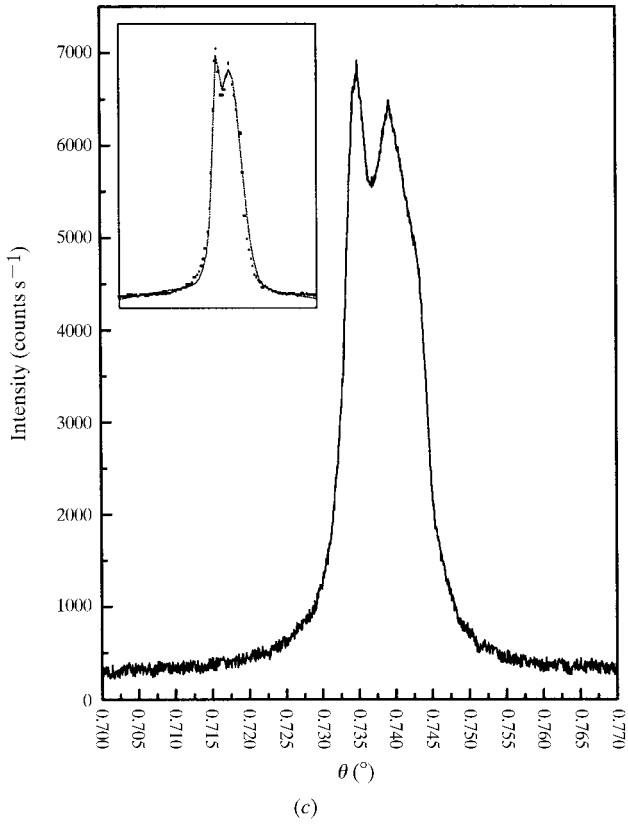

Figure 4
Rocking curves acquired from the crystal in Fig. 2 at different times (as indicated in Fig. 3). These times are 47.5, 53 and 70 h, respectively. The insets in all plots show the profile fitting used to estimate the contribution of different domains to the whole profile. Vertical scales (in counts s^{-1}) are different.

the growth rate, *i.e.* the time derivative of the previous curve. After an initial transient regime of low growth rate shortly after nucleation, the growth rate reaches a maximum and then starts to decrease, asymptotically approaching zero. This growth rate can be mapped onto the sequence of crystal profiles shown in Fig. 2, in which the varying growth-rate layers which make up the crystal are evident (inset in Fig. 3). As a result, the crystal has a relatively small core, grown at a low rate, around which there is a volume which grew at greater rates and then another zone (mostly composed of the left and right parts of the cylindrical crystal) again grown at a low rate.

If, as expected, crystal-growth rate controls the quality of the resulting crystal, we have to recover this distribution in time and space for the mosaicity values. Fig. 4 shows a series of peaks recorded from the crystal in Fig. 2 during the experiment before (47.5 h), close to (53 h) and after (70 h) the maximum growth rate. Peaks are drawn at different vertical scales. FWHM values are, respectively 23, 53 and 41 arcsec (6.4×10^{-3}, 14.7×10^{-3} and 11.4×10^{-3}°), supporting the influence of growth rate on crystal quality. The relative importance of each domain is represented by the relative area (integrated intensity) of the corresponding peak: from the beginning (Fig. 4*a*) two domains appear as two different peaks above a much wider one. At this stage, the peak on the left is one order of magnitude higher than the peak on the right. Further growth of the crystal (Fig. 4*b*) produces a widening of the peak owing to the development of the right peak and the wide third peak. At this stage, the intensity ratio has changed because the integrated intensity of the right peak rises quickly owing to the different development of the volumes of each domain. Later (Fig. 4*c*), both peaks present a comparable integrated intensity and they both grow, while the wide peak does not change, resulting in a reduction of the FWHM.

The spatial distribution of these different domains was recorded using topography, which confirms that the two peaks correspond mainly to the two ends of the crystal in the direction of the capillary, while a much lower intensity zone is observed around the initial core. This fact was also confirmed by illuminating only the outer (top in Fig. 1) part of the crystal by closing the slits; note that this part excludes almost all the crystal volume close to the initial core. In doing so, both peaks are well separated (Fig. 5) because the middle wider peak corresponding to the volume around the core is not illuminated, and a very low value of FWHM (9.2 arcsec for the left peak and 12.8 arcsec for the right peak) can be measured for the two slowly growing ends of the crystal. These results show the existence of a clear distribution of mosaicity values during the crystal growth and (consequently) throughout the crystal volume, with a lower quality (higher mosaic spread) for the parts of the crystal that grow quickly at the beginning of the experiment (at the centre of the crystal) and lower mosaicity values for the outer parts, according to their lower growth rate.

Compared with profiles recorded from stabilized crystals grown in our laboratory and taken to LURE, the profiles from crystals grown *in situ* show differences, especially in the overall peak shape: more Gaussian-like (almost single domain) peaks were observed in crystals grown during the experiment than in crystals brought from our laboratory. This difference is not so definitive when considering the FWHM of peaks, where similar or even larger values were found in the *in-situ* grown crystals. The most reasonable explanation for this seems to be the absence of mechanical stress in *in situ* grown crystals which implies a better domain distribution (more Gaussian-like peaks), although FWHM values, mainly controlled by the growth rate, are larger in the *in-situ* grown crystals owing to the higher supersaturation at which these crystals were grown. This higher supersaturation was selected as a consequence of time constraints. The time assigned to this experiment (5 d) was much shorter than the time requested. In order to obtain several crystals of reasonable size after 5 d, we were forced to use higher protein concentrations than we usually use in our laboratory to push the growth rate to a value sufficient for growing the crystals in the time available. New experiments were prepared during 1998 with more beamtime and different timings in order to observe crystals growing at lower supersaturation values, of the same order as those already optimized in our laboratory.

4. Conclusions

The mosaic spread in protein crystals is not a homogeneous property over the crystal volume, but varies for different parts of the crystal. These variations arise from the different development of crystal volumes having different local mosaic spread. The parts of the crystal with largest volume contri-

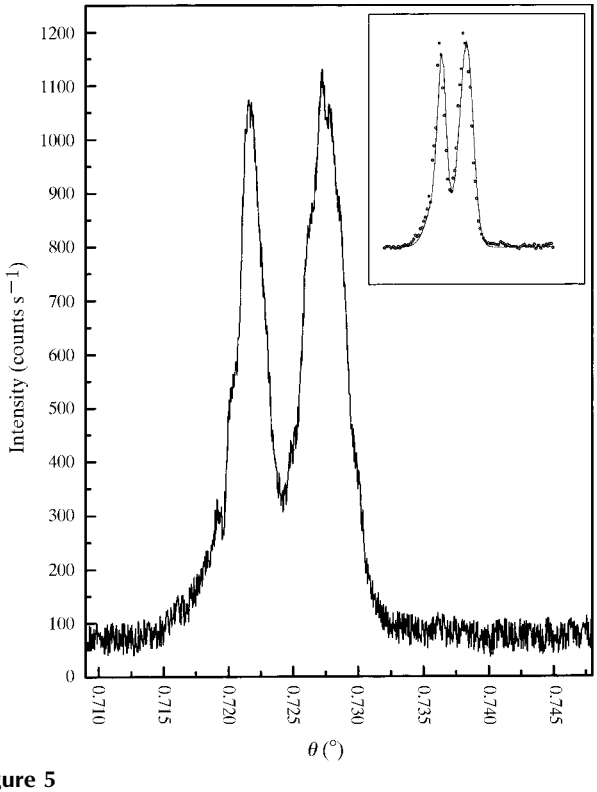

Figure 5
Rocking curve from a small volume at the periphery of the crystal after 98 h. This volume is composed almost completely of two domains with FWHM 9.2 and 12.8″.

butions from domains showing narrow rocking curves present lowest mosaicity values. This domain distribution, which produces the observed mosaicity distribution in time and space, is a direct consequence of the varying growth rate during crystal growth. Further handling of the crystals produces widening of the peaks owing to mechanical stress, which is avoided with the experimental setup discussed in this paper.

This study was carried out with financial support from the Spanish Ministerio de Educación y Cultura project PB-0220. Travel and accommodation expenses during experiments were met by LURE.

References

Ferrer, J. L., Hirschler, J., Roth, M. & Fontecilla-Camps, J. C. (1996). *ESRF Newslett.* June 1996, pp. 27–29.

Fourme, R., Ducruix, A., Riès-Kautt, M. & Capelle, B. (1995). *J. Synchrotron Rad.* **2**, 136–142.

García-Ruiz, J. M. & Moreno, A. (1994). *Acta Cryst.* D**50**, 483–490.

García-Ruiz, J. M., Moreno, A., Otálora, F., Viedma, C., Rondón, D. & Zautscher, F. (1998). *J. Chem. Ed.* **75**, 442–446.

García-Ruiz, J. M., Moreno, A., Parraga, A. & Coll, M. (1995). *Acta Cryst.* D**51**, 278–281.

García-Ruiz, J. M., Moreno, A., Viedma, C. & Coll, M. (1993). *Mater. Res. Bull.* **28**, 541–546.

García-Ruiz, J. M. & Otálora, F. (1997). *J. Cryst. Growth*, **182**, 155–167.

Helliwell, J. R. (1988). *J. Cryst. Growth*, **90**, 259–272.

Helliwell, J. R., Snell, E. & Weisgerber, S. (1995). In *Proceedings of the IXth European Symposium on Gravity Dependent Phenomena in Physical Sciences*, edited by L. Ratke, H. Walter & B. Feuerbacher. Berlin: Springer Verlag.

Moreno, A., Rondón, D. & García-Ruiz, J. M. (1996). *J. Cryst. Growth*, **166**, 919–924.

Otálora, F., Capelle, B., Ducruix, A. & García-Ruiz, J. M. (1999). *Acta Cryst.* D**55**, 644–649.

Otálora, F. & García-Ruiz, J. M. (1996). *J. Cryst. Growth*, **169**, 361–367.

Otálora, F., García-Ruiz, J. M. & Moreno, A. (1996). *J. Cryst. Growth*, **168**, 93–98.

Riès-Kautt, M., Broutin, I., Ducruix, A., Shepard, W., Kahn, R., Chayen, N., Blow, D., Paal, K., Littke, W., Lorber, B., Theobald-Dietrich, A. & Giegé, R. (1997). *J. Cryst. Growth*, **181**, 79.

Snell, E. H., Weisgerber, S., Helliwell, J. R., Weckert, E., Hölzer, K. & Schroer, K. (1995). *Acta Cryst.* D**51,** 1099–1102.

Vaney, M. C., Maignan, S., Riès-Kautt, M. & Ducruix, A. (1996). *Acta Cryst.* D**52**, 505–517.